

Contribution from the Scientific Research Staff, Ford Motor Company, Dearborn, Michigan 48121, and the Department of Chemistry, The University of Michigan, Ann Arbor, Michigan 48109

Rhodium and Iridium Complexes of Biimidazole. 2. Tetranuclear Carbonyl Derivatives

S. W. KAISER, R. B. SAILLANT, W. M. BUTLER, and P. G. RASMUSSEN*

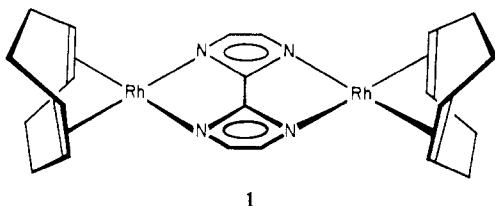
Received March 9, 1976

AIC601885

Carbonyl complexes of univalent rhodium and iridium containing the dianion of 2,2'-biimidazole have been investigated. The syntheses and characterizations of $M_4(CO)_8(BiIm)_2$ (where $M = Rh(I), Ir(I)$, $BiIm = 2,2'$ -biimidazole dianion) are described herein. The intermediate composition in the rhodium case $Rh_4(COD)_2(CO)_4(BiIm)_2$ ($COD = 1,5$ -cyclooctadiene) has also been isolated. Inequivalent ring hydrogens as shown by 1H NMR spectra, inequivalent carbonyl groups as shown by ir spectra, and a solution molecular weight all indicated a molecular complexity for $M_4(CO)_8(BiIm)_2$ belied by the empirical formula. The structural problem was solved by a three-dimensional, single-crystal x-ray diffraction study on $Rh_4(CO)_8(BiIm)_2$, done by counter methods. The red complex of $Rh_4C_{20}H_8O_8N_8$ was found to crystallize in the orthorhombic space group *Pbcn* with $a = 15.034$ (3) Å, $b = 8.257$ (1) Å, $c = 20.891$ (4) Å, and $Z = 4$ molecules/cell. The structure was refined by full-matrix methods to $R = 0.032$ and $R_w = 0.038$ for 1771 nonzero reflections. The tetranuclear structure, suggested by the solution molecular weight, persists in the solid state and has several novel features. The V-shaped complex is better written as $(CO)_2Rh(BiIm)[Rh_2(CO)_4](BiIm)Rh(CO)_2$ where the pair of rhodium atoms are at the bottom of the V. The biimidazole dianions are each bidentate to the terminal rhodiums and unidentate to each of the bridging rhodiums. The latter rhodiums have the closest known $Rh(I)-Rh(I)$ distance 2.975 (1) Å. The biimidazole dianions are roughly planar and lie parallel to the coordination planes of the terminal rhodiums and perpendicular to the coordination planes of the bridging rhodiums. The latter planes have typical square-planar parameters except for the metal-metal bond. The four carbonyl ligands point down from the bottom of the V and are staggered about the $Rh-Rh$ axis by approximately 40° . The "sawtooth" packing may be viewed as infinite chains of alternating V's along the c axis, viz., VAVA, etc. The intermolecular distance between terminal $Rh(I)$ atoms is 3.259 (2) Å. The novel coordination exhibited by the biimidazole dianion bridge in this structure is discussed.

Introduction

The selective preparation of rhodium(I) and iridium(I) complexes with the monoanion and dianion of 2,2'-biimidazole (H_2BiIm) has been described.¹ The x-ray crystal structure of $Rh_2(COD)_2(BiIm)$, **1**, where COD is 1,5-cyclooctadiene



and $BiIm$ is the dianion of 2,2'-biimidazole, has been solved.¹ The dianion coordinates in a symmetrical manner as a quadridentate ligand with two rhodium(I) atoms forming a strictly planar $Rh_2(BiIm)$ unit.

This paper describes the synthesis and characterization of rhodium(I) and iridium(I) carbonyl complexes with the dianion of 2,2'-biimidazole. This work was undertaken in an attempt to form extended planar systems with low steric requirements out of plane. These arrays were designed to allow stacking in the solid state with parallel planes, permitting interaction between the metal atoms. The physical properties of such systems, e.g., highly anisotropic conductivity, have been reviewed.² Through replacement of the terminal COD ligands in **1** with sterically compact carbonyl ligands, a novel dimeric stacking unit was anticipated. However, ir and NMR data, previously communicated,³ were not consistent with a simple analogue of **1**. We now report the crystal structure of $Rh_4(CO)_8(BiIm)_2$, assigned earlier as $Rh_2(CO)_4(BiIm)$.³

Experimental Section

Unless otherwise noted, all syntheses and solution manipulations of rhodium(I) and iridium(I) complexes were performed with Schlenk-type apparatus under argon. The argon was purified by filtration through successive columns of heated BASF catalyst R3-11, Drierite, and P_2O_5 . All reactions were nearly quantitative with absolute yield being limited by recovery losses.

Reagents. Reagent grade solvents were deaerated and stored over molecular sieves (Linde Type 4-A) or freshly distilled from calcium hydride under purified argon. $Rh(COD)(HBiIm)$,¹ $Rh(CO)_2-$

$(HBiIm)$,¹ $M_2(COD)_2(BiIm)$,¹ $Rh(COD)(acac)$ ⁴ (using the method described for Ir analogue where $acac$ is the anion of acetylacetonate), and H_2BiIm ¹ were prepared by methods previously described. The remaining compounds were purchased from the indicated commercial sources: $Rh(CO)_2(acac)$, Strem Chemicals, Inc.; $Ir(CO)_2(acac)$, Pressure Chemical Co.; 90% enriched ^{13}C and deuterated NMR solvents, Stohler Isotope Co.

Physical Measurements. Infrared spectra between 4000 and 250 cm^{-1} were recorded on a Perkin-Elmer Model 457 grating spectrophotometer. The samples were suspended in KBr pellets or Nujol mulls placed between KBr plates. Routine solution spectra of the carbonyl stretching region were recorded on a Perkin-Elmer Model 237 spectrophotometer. Carbonyl stretching frequencies accurate to ± 0.5 cm^{-1} between 2100 and 1800 cm^{-1} were obtained on a Perkin-Elmer Model 180 infrared spectrophotometer. The grating was calibrated from water vapor modes at 1889.6, 1869.4, and 1844.2 cm^{-1} . Solutions of the samples were contained in a 0.57-mm cell with CaF_2 windows with neat solvent in a matching cell as a reference.

Proton NMR spectra were recorded on Bruker HX-60 and Jeolco JNM-PS-100 spectrometers, both equipped with variable-temperature probes. Due to low solubility of the complexes 10-mm diameter sample tubes were used in the Bruker HX-60 probe with TMS as a reference and a lock signal. The Jeolco instrument was operated with 4-mm diameter tubes, a deuterium lock signal obtained from the deuterated solvent, and a TMS reference signal. Probe temperatures in both instruments were calibrated with methanol below ambient temperature and ethylene glycol above ambient temperature. The calibration temperature was obtained from graphs of a specific chemical shift for each standard vs. temperature as supplied with each instrument.

Proton-decoupled ^{13}C NMR spectra were obtained on the Jeolco JNM-PS-100 spectrometer described above operating in the pulsed Fourier transform mode. Again 4-mm diameter sample tubes, a deuterium lock signal, and a TMS reference signal were used. Tris(acetylacetonato)chromium (0.05 M) was added as a shiftless relaxation agent⁵ to shorten the long T_1 relaxation times associated with metal-bonded carbonyl carbons.

Low-resolution mass spectral services were performed by Shrader Analytical and Consulting Laboratories, Inc., Detroit, Mich. 48210. The solid sample was introduced directly into the ionization chamber.

Elemental analyses were performed by Spang Microanalytical Laboratory, Ann Arbor, Mich. 48106.

Solution molecular weights in methylene chloride at 39 ± 0.2 °C were determined by the Singer isopiestic method.⁶ $[Rh(COD)Cl]_2$, mol wt 493 in solution,⁷ was used as the standard.

The dc electrical resistivities on compressed powders and single crystals were measured by the two-probe method using Aquadag contacts (Acheson Colloids, Port Huron, Mich.). A 5-V battery

* To whom correspondence should be addressed at the University of Michigan.

through a series of decade resistors was used as the current source. The voltage drop across the sample vs. current was displayed on a dual-beam Tektronix Model 502 oscilloscope in order to determine the ohmic behavior of the contacts.

Preparation of $\text{Rh}_4(\text{COD})_2(\text{CO})_4(\text{BiIm})_2$. Method A. $\text{Rh}(\text{COD})(\text{HBiIm})$, 200 mg (0.581 mmol), was added to 30 ml of benzene with stirring. The mixture was warmed and stirred for 10 min to dissolve as much complex as possible. After cooling of the mixture to room temperature, 150 mg (0.582 mmol) of $\text{Rh}(\text{CO})_2\text{acac}$ was added in four portions over 10 min. All $\text{Rh}(\text{COD})(\text{HBiIm})$ dissolved and the solution turned dark red. The solution was stirred for 10 min and filtered, and 20 ml of solvent was removed under reduced pressure. An orange-red microcrystalline solid formed and was collected by filtration. Anal. Calcd for $\text{C}_{32}\text{H}_{32}\text{N}_8\text{O}_4\text{Rh}_4$: C, 38.27; H, 3.21; N, 11.16. Found: C, 38.89; H, 3.27; N, 11.04.

Method B. $\text{Rh}(\text{COD})(\text{acac})$, 106 mg (0.342 mmol), was added in four portions over 10 min to a stirred suspension of $\text{Rh}(\text{CO})_2(\text{HBiIm})$, 100 mg (0.342 mmol), in 30 ml of benzene. All $\text{Rh}(\text{CO})_2(\text{HBiIm})$ dissolved with formation of a dark red solution. After being stirred for 10 min, the solution was filtered and 20 ml of solvent was removed under reduced pressure. The orange-red microcrystalline solid was isolated and identified as $\text{Rh}_4(\text{COD})_2(\text{CO})_4(\text{BiIm})_2$ by comparison of its infrared spectrum with that of an authentic sample.

Preparation of $\text{Rh}_4(\text{CO})_8(\text{BiIm})_2$. Method A. Carbon monoxide was passed through a suspension of 250 mg (0.451 mmol) of $\text{Rh}_2(\text{COD})_2(\text{BiIm})$ in 40 ml of benzene for 30 min. After 15 min all $\text{Rh}_2(\text{COD})_2(\text{BiIm})$ had reacted forming a red solution. Gradually, an orange-red solid formed. The solution was concentrated under reduced pressure and cooled, and the red microcrystalline solid was collected by filtration. Anal. Calcd for $\text{C}_{20}\text{H}_8\text{O}_8\text{N}_8\text{Rh}_4$: C, 26.60; H, 0.90; N, 12.45. Found: C, 26.93; H, 1.20; N, 12.51.

Method B. $\text{Rh}(\text{CO})_2(\text{acac})$, 200 mg (0.776 mmol), and an excess of H_2BiIm , 100 mg (0.746 mmol), were added to 30 ml of benzene with stirring. The mixture was heated to reflux for 1 h with formation of a red-orange solution. The mixture was cooled and filtered to collect the excess H_2BiIm , 48 mg (0.358 mmol). The filtrate was then concentrated to 10 ml. The orange-red microcrystalline material was collected by filtration and confirmed as $\text{Rh}_4(\text{CO})_8(\text{BiIm})_2$ by comparison of the ir spectrum with that of an authentic sample.

Method C. Carbon monoxide was passed through a benzene solution of $\text{Rh}_2(\text{COD})(\text{CO})_2(\text{BiIm})$ for 5 min. The orange-red solid which formed was isolated and identified as $\text{Rh}_4(\text{CO})_8(\text{BiIm})_2$ by comparison of the ir spectrum with that of an authentic sample.

Preparation of $\text{Ir}_4(\text{CO})_8(\text{BiIm})_2$. Method B described above for $\text{Rh}_4(\text{CO})_8(\text{BiIm})_2$ was employed to prepare this complex using $\text{Ir}(\text{CO})_2(\text{acac})$, 250 mg (0.720 mmol), H_2BiIm , 100 mg (0.746 mmol), and 30 ml of methylene chloride. A reddish purple solution was obtained with formation of nearly black needles upon concentration of the filtrate under a stream of argon. Anal. Calcd for $\text{C}_{20}\text{H}_8\text{N}_8\text{O}_8\text{Ir}_4$: C, 19.11; H, 0.64; N, 8.91. Found: C, 19.33; H, 0.80; N, 8.47.

Preparation of $\text{Rh}_4(^{13}\text{CO})_8(\text{BiIm})_2$. A sample of 100 mg of $\text{Rh}_4(\text{CO})_8(\text{BiIm})_2$ in 20 ml of benzene was stirred under an atmosphere of ^{13}CO for 6 h. The solvent was then removed under reduced pressure and the substituted product was isolated.

Crystal Structure Determination of $\text{Rh}_4(\text{CO})_8(\text{BiIm})_2$

Data Collection and Reduction. Single crystals of $\text{Rh}_4(\text{CO})_8(\text{BiIm})_2$ were obtained by slow evaporation of a toluene solution of the complex contained in a Nalgene vessel (to prevent solvent creep) using carbon monoxide as the flow gas. The experimental density was determined by flotation in a solution of carbon tetrachloride and methylene bromide. A summary of data collection and crystal parameters is given in Table I.

A single crystal suitable for data collection was mounted directly on a Syntex PI four-circle diffractometer. Rotation and axial photographs and counter data indicated the space group $Pbcn$ which was later confirmed by successful solution of the structure. Fifteen reflections were centered using a programmed centering routine. Cell constants and errors were obtained by least-squares refinement of these angular settings. The orientation matrix required for subsequent data collection was calculated.

Intensity data were collected using Mo $K\alpha$ radiation monochromatized from a graphite crystal whose diffraction vector was perpendicular to the diffraction vector of the sample. The θ - 2θ scan technique was used with variable scan rate determined as a function

Table I. Summary of Crystal Data and Intensity Collection for $\text{Rh}_4(\text{CO})_8(\text{BiIm})_2$

Space group	$Pbcn$
a , Å	15.034 (3)
b , Å	8.257 (1)
c , Å	20.891 (4)
$\alpha = \beta = \gamma$, deg	90
V , Å ³	2593.2
Mol wt	449.974
Z	4
d_{obsd} , g/cm ³	2.317 (5)
d_{calcd} , g/cm ³	2.305
Crystal dimensions (interfacial), mm	0.15-0.24
Crystal shape	Pseudooctahedron
Radiation, Å	$\lambda(\text{Mo } K\alpha)$ 0.710 69, monochromatized from oriented graphite crystal
Takeoff angle, deg	4.0
Linear absorption coeff, μ , cm ⁻¹ (Mo $K\alpha$)	25.04
Transmission factors	0.66-0.72
Scan speed, deg/min	Variable, 1.5-15, determined as a function of peak intensity
Scan range, 2θ , deg	Mo $K\alpha_1$ - 0.9 to Mo $K\alpha_2$ + 0.8
Ratio of background time to peak scan time	0.8
Std reflections	(200), (020), (002)
Dev of standards during data collection	<5%
2θ limit, deg	55
Reflections collected	3422
Reflections with $F^2 > 3\sigma(F^2)$	1771

of peak intensity in order to obtain comparable counting statistics. Backgrounds were measured at each end of the scan for a total time equal to 0.8 of the scan time. During data collection, the intensities of three standard reflections were measured every 50 reflections. Fluctuations were less than 5%.

The data were reduced by procedures similar to those previously described.⁸ Standard deviations were assigned as

$$\sigma(I) = [\sigma_{\text{counter}}I^2 + (0.04I)^2]^{1/2}$$

where $\sigma_{\text{counter}} = (I + K^2B)^{1/2}$, I is the net intensity, B is the total background counting time, and K is the ratio of scan time to background time. The data were not corrected for absorption due to the small difference between maximum and minimum values of the transmission factors.⁸ A set of reflections representing diverse cross sections of the crystal was chosen for trial absorption calculations. Only those data for which $F^2 \geq 3\sigma(F^2)$ were used in the structure solution and refinement.

Solution and Refinement of the Structure. Atomic scattering factors for nonhydrogen atoms were taken from Cromer and Waber's compilation.⁹ Those for hydrogen and anomalous dispersion correction terms $\Delta f'$ and $\Delta f''$ due to rhodium were obtained from ref 10.

The agreement indices are defined as

$$R = \sum [|F_o| - |F_c|] / \sum |F_o|$$

$$R_w = [\sum w(|F_o| - |F_c|)^2 / \sum w F_o^2]^{1/2}$$

where F_o and F_c are the observed and calculated structure factors, respectively. The factor minimized during refinement was $\sum w(|F_o| - |F_c|)^2$. The average deviation in an observation of unit weight is defined as $[w(|F_o| - |F_c|)^2 / (m - n)]^{1/2}$ where m is the number of reflections and n is the number of refined parameters.

This structure was solved by conventional Patterson and Fourier syntheses.⁸ From the initial three-dimensional Patterson map, the atomic coordinates of the two rhodium atoms per asymmetric unit were obtained. These heavy-atom positions and assigned isotropic temperature factors were refined with one least-squares cycle and used to phase the structure factors ($R = 0.28$, $R_w = 0.33$). Residuals around 30% indicated the probable correctness of the model. A difference Fourier electron density map was calculated using the rhodium contributions. All nonhydrogen atoms of the asymmetric unit were then located. Two cycles of least-squares refinement of the scale factor

Table II. Final Position Parameters for $\text{Rh}_4(\text{CO})_8(\text{BiIm})_2^a$

Atom	<i>x</i>	<i>y</i>	<i>z</i>
Rh(1)	0.097 90 (3)	0.171 31 (6)	0.260 37 (2)
Rh(2)	-0.035 84 (4)	0.643 55 (6)	0.453 08 (2)
O(1)	0.089 8 (5)	0.010 2 (8)	0.387 7 (3)
O(2)	0.103 3 (4)	-0.154 4 (7)	0.198 8 (3)
O(3)	0.085 4 (4)	0.875 7 (6)	0.520 3 (3)
O(4)	-0.188 0 (4)	0.722 4 (8)	0.538 5 (3)
N(1)	0.087 3 (3)	0.394 9 (6)	0.306 0 (2)
N(2)	0.053 5 (3)	0.575 2 (6)	0.381 5 (2)
N(3)	0.117 3 (3)	0.291 4 (6)	0.174 7 (2)
N(4)	0.110 2 (3)	0.478 2 (6)	0.097 3 (2)
C(1)	0.092 8 (5)	0.067 9 (8)	0.339 0 (4)
C(2)	0.105 2 (5)	-0.030 8 (9)	0.220 7 (3)
C(3)	0.039 3 (6)	0.789 8 (8)	0.494 7 (3)
C(4)	-0.128 3 (6)	0.693 9 (9)	0.507 5 (3)
C(5)	0.067 1 (4)	0.400 8 (7)	0.144 7 (3)
C(6)	0.024 3 (4)	0.450 2 (7)	0.345 5 (3)
C(7)	0.194 8 (5)	0.412 3 (9)	0.097 8 (3)
C(8)	0.198 5 (4)	0.297 6 (9)	0.143 9 (3)
C(9)	0.161 3 (5)	0.493 0 (9)	0.316 3 (3)
C(10)	0.140 7 (5)	0.600 4 (9)	0.364 2 (3)

^a Standard deviation for the last significant digit is given in parentheses.

and individual positional and isotropic thermal parameters led to convergence with $R = 0.079$ and $R_w = 0.097$. Continued refinement using anisotropic thermal parameters for all nonhydrogen parameters led to convergence with $R = 0.035$ and $R_w = 0.043$. A difference-Fourier synthesis revealed the positions of the four hydrogen atoms of the BiIm ring. Fixed hydrogen atom contributions to the structure factors were included in subsequent refinements. Hydrogen atom coordinates were calculated⁸ assuming carbon-hydrogen distances of 0.95 Å in idealized trigonal-planar geometry. Fixed isotropic temperature factors were assigned as one unit larger than the carbon to which the hydrogen atom was bonded, i.e., $B_{\text{H}} = [B_{\text{C}} + 1.0] \text{ \AA}^2$. Two cycles of least-squares refinement of positional parameters and anisotropic thermal parameters for all nonhydrogen atoms with fixed hydrogen atom contributions led to final convergence with $R = 0.032$ and $R_w = 0.038$. Refinement was ceased when no individual parameter shift greater than 0.20 that of the corresponding estimated standard deviation was observed. The average deviation in an observation of unit weight was 1.22. The number of reflections (m) was 1771 and the number of variables (n) was 181 giving an $m:n$ ratio 9.5:1. In the final difference Fourier map no peak greater than 0.51 e \AA^{-3} was observed.

Final nonhydrogen positional and thermal parameters are collected in Tables II and III, respectively. Calculated hydrogen atom coordinates and fixed isotropic thermal parameters are given in Table IV. A listing of observed and calculated structure factor amplitudes

is available. (See paragraph at end of paper regarding supplementary material.)

Characterization

The complex $\text{Rh}_4(\text{CO})_8(\text{BiIm})_2$, **2**, is readily obtained as a red microcrystalline material, when carbon monoxide is passed through a benzene solution of $\text{M}_2(\text{COD})_2(\text{BiIm})$, displacing the diene. This material is air stable and slightly soluble in dry, deoxygenated organic solvents. Solutions of $\text{Rh}_4(\text{CO})_8(\text{BiIm})_2$ rapidly decompose when exposed to air forming uncharacterized products.

The complexes $\text{M}_4(\text{CO})_8(\text{BiIm})_2$ may also be prepared conveniently by treating $\text{M}(\text{CO})_2(\text{acac})$ with a small excess of H_2BiIm . In contrast to reactions of $[\text{M}(\text{COD})(\text{OMe})]_2$ with 2 mol of H_2BiIm (forming the monoanion),¹ only complexes containing the dianion are obtained with acac^- , regardless of molar ratios. $\text{Ir}_4(\text{CO})_8(\text{BiIm})_2$, **3**, is obtained most easily by this method and is isolated as nearly black needles. The material, however, decomposes in the solid state when exposed to air. It is slightly soluble in dry, deoxygenated organic solvents and its solutions also rapidly decompose when exposed to air. The decomposition products have not been characterized.

The mixed-ligand complex $\text{Rh}_4(\text{CO})_4(\text{COD})_2(\text{BiIm})_2$, **4**, is obtained by treating $\text{Rh}(\text{COD})(\text{HBiIm})$ with 1 mol of $\text{Rh}(\text{CO})_2(\text{acac})$ or by treating $\text{Rh}(\text{CO})_2(\text{HBiIm})$ with 1 mol of $\text{Rh}(\text{COD})(\text{acac})$. Thus, the mononuclear complex containing the monoanion is used as an intermediate in the stepwise formation of the dianion complex. Reactions of the mononuclear complex with reagents containing methoxide as the base under identical reaction conditions yielded $\text{Rh}_2(\text{COD})_2(\text{BiIm})$ and $\text{Rh}_4(\text{CO})_8(\text{BiIm})_2$, again demonstrating the dependence of the product of reaction on the base used. The complex forms as air-stable, red microcrystals. The substance is slightly soluble in dry, deoxygenated organic solvents; these solutions readily decompose upon exposure to air forming uncharacterized products. The COD ligands are readily displaced by passing CO through a solution of the complex, thus forming $\text{Rh}_4(\text{CO})_8(\text{BiIm})_2$.

The infrared absorption of the BiIm^{2-} regions of **2-4** generally resemble those observed for $\text{M}_2(\text{COD})_2(\text{BiIm})$.¹ However distinct differences exist between the carbonyl complexes and the cyclooctadiene complexes.¹ The most intense band in the 1500–1400- cm^{-1} region (ring stretching) shifts from 1465 cm^{-1} for **1** to 1400 cm^{-1} for **2-4**. Likewise, in the 1150–1100- cm^{-1} region (in-plane C–H bending) the

Table III. Final Anisotropic Thermal Parameters for $\text{Rh}_4(\text{CO})_8(\text{BiIm})_2^{a,b}$

Atom	β_{11}	β_{22}	β_{33}	β_{12}	β_{13}	β_{23}
Rh(1)	26.5 (2)	115.2 (7)	15.2 (1)	8.1 (4)	0.0 (1)	-3.0 (3)
Rh(2)	48.7 (3)	103.2 (7)	14.4 (1)	17.9 (4)	1.6 (2)	-1.2 (3)
O(1)	145 (6)	211 (11)	24 (2)	-8 (7)	5 (3)	25 (4)
O(2)	75 (4)	181 (10)	49 (2)	10 (5)	5 (2)	-48 (4)
O(3)	87 (4)	143 (9)	29 (2)	9 (5)	-12 (2)	-7 (3)
O(4)	74 (4)	313 (15)	34 (2)	50 (6)	18 (2)	-21 (4)
N(1)	33 (3)	116 (8)	16 (1)	-5 (4)	2 (2)	-6 (3)
N(2)	36 (3)	121 (8)	16 (1)	1 (4)	1 (2)	-3 (3)
N(3)	30 (2)	123 (8)	15 (1)	4 (4)	2 (1)	-1 (3)
N(4)	38 (3)	135 (9)	16 (1)	-11 (4)	2 (2)	-6 (3)
C(1)	53 (4)	124 (11)	22 (2)	-1 (6)	0 (3)	-6 (4)
C(2)	36 (3)	171 (13)	23 (2)	11 (6)	2 (2)	-13 (4)
C(3)	69 (5)	105 (10)	16 (2)	20 (6)	-1 (2)	3 (3)
C(4)	62 (4)	163 (13)	18 (2)	33 (6)	-2 (2)	-10 (4)
C(5)	32 (3)	121 (10)	14 (1)	-8 (5)	3 (2)	-8 (3)
C(6)	36 (3)	98 (9)	14 (1)	8 (4)	1 (2)	2 (3)
C(7)	36 (4)	170 (13)	21 (2)	-14 (5)	5 (2)	-18 (4)
C(8)	31 (3)	150 (12)	19 (2)	2 (5)	2 (2)	-7 (4)
C(9)	34 (3)	149 (11)	22 (2)	-17 (5)	2 (2)	-8 (4)
C(10)	40 (4)	143 (12)	23 (2)	-14 (5)	-2 (2)	-9 (4)

^a All values multiplied by 10^4 . Standard deviation for the last significant digit(s) is given in parentheses. ^b The form of the anisotropic thermal parameter is $\exp[-(h^2\beta_{11} + k^2\beta_{22} + l^2\beta_{33} + 2hk\beta_{12} + 2hl\beta_{13} + 2kl\beta_{23})]$.

Table IV. Calculated Hydrogen Atom Positions and Assigned Isotropic Thermal Parameters for $\text{Rh}_4(\text{CO})_8(\text{BiIm})_2$

Atom	x	y	z	B, Å ²
H(7) ^a	0.2424	0.4426	0.0704	4.8
H(8)	0.2486	0.2320	0.1535	4.4
H(9)	0.2163	0.4866	0.2941	4.7
H(10)	0.1798	0.6785	0.3821	4.8

^a Number refers to carbon atom to which the hydrogen is bonded.

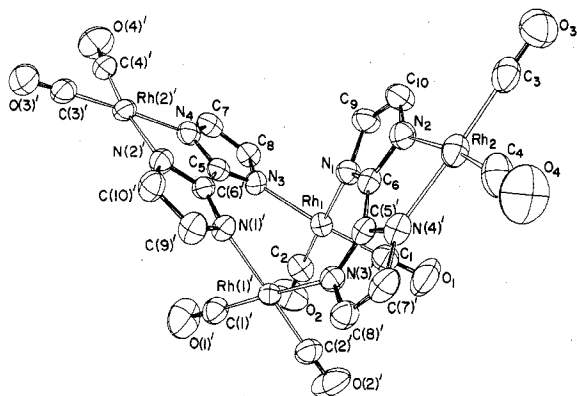


Figure 1. The molecular structure of $\text{Rh}_4(\text{CO})_8(\text{BiIm})_2$. The asymmetric unit $\text{Rh}_2(\text{CO})_4(\text{BiIm})$ is depicted by the unprimed atoms.

most intense band shifts from 1118 to 1135 cm^{-1} .

The solution ir of the carbonyl stretching region and the NMR spectra of **2** and **3** showed unexpected complexity. Chemically inequivalent ring protons and carbonyl groups were confirmed by ¹³C enrichment. These ¹H NMR, ¹³C NMR, and ir shifts have been previously described.¹

In the low-resolution mass spectrum of **2**, no parent molecular ion or fragments greater than m/e 200 were observed in contrast to $\text{Rh}_2(\text{COD})_2(\text{BiIm})$ for which the parent ion was observed.¹ Due to the low solubility of the complexes and the sensitivity of their solutions to air, the determination of solution molecular weight by osmometric methods was not possible. However, a solution molecular weight of 875 ± 50 for the rhodium carbonyl complex was obtained by the Singer isopiestic method.⁶

The solution of the x-ray crystal structure of the rhodium carbonyl complex **2** was undertaken in order to resolve the problems raised by these results.

Description of the Structure

The molecular geometry of the tetranuclear complex $\text{Rh}_4(\text{CO})_8(\text{BiIm})_2$ is shown in Figure 1. The asymmetric unit, $\text{Rh}_2(\text{CO})_4(\text{BiIm})$, is depicted by unprimed atom labels in Figure 1. The second half of the molecule is related by a crystallographic twofold axis normal to the line joining $\text{Rh}(1)-\text{Rh}(1)'$. A stereoscopic view of the molecule is given in Figure 2. The biimidazole ligand coordinates simultaneously in a bidentate manner through both imidazole rings to one rhodium atom and also in a monodentate manner

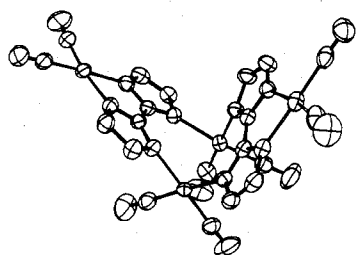


Figure 2. Stereoview of $\text{Rh}_4(\text{CO})_8(\text{BiIm})_2$.

Table V. Intramolecular Bond Lengths for $\text{Rh}_4(\text{CO})_8(\text{BiIm})_2$ ^a

Bond	Length, Å	Bond	Length, Å
Ring 1			
Rh(1)-N(1)	2.084 (5)	Rh(1)-N(3)	2.067 (5)
Rh(2)-N(2)	2.087 (5)	Rh(2)-N(4)'	2.055 (5)
N(1)-C(9)	1.392 (8)	N(3)-C(8)	1.380 (7)
C(9)-C(10)	1.372 (9)	C(8)-C(7)	1.352 (10)
C(10)-N(2)	1.378 (9)	C(7)-N(4)	1.384 (8)
N(2)-C(6)	1.351 (7)	N(4)-C(5)	1.344 (7)
C(6)-N(1)	1.336 (7)	C(5)-N(3)	1.333 (8)
Ring 1-Ring 2			
Rh(1)-Rh(1)'	2.975 (1)	N(2)-N(4)'	2.625 (7)
C(5)-C(6)'	1.449 (9)	N(1)-N(3)'	3.218 (7)
Carbonyl Ligands			
Rh(1)-C(1)	1.852 (7)	C(1)-O(1)	1.124 (8)
Rh(1)-C(2)	1.866 (7)	C(2)-O(2)	1.119 (8)
Rh(2)-C(3)	1.870 (8)	C(3)-O(3)	1.127 (8)
Rh(2)-C(4)	1.843 (8)	C(4)-O(4)	1.131 (9)

^a Standard deviation for the last significant digit(s) is given in parentheses.

Table VI. Intramolecular Angles for $\text{Rh}_4(\text{CO})_8(\text{BiIm})_2$ ^a

Atoms	Angle, deg	Atoms	Angle, deg
About Rh(1)			
N(3)-Rh(1)-N(1)	89.0 (2)	About Rh(2)	
N(1)-Rh(1)-C(1)	90.0 (2)	N(2)-Rh(2)-N(4)'	78.7 (2)
C(1)-Rh(1)-C(2)	89.1 (3)	N(2)-Rh(2)-C(3)	96.9 (3)
C(2)-Rh(1)-N(3)	92.1 (3)	C(3)-Rh(2)-C(4)	91.3 (3)
C(1)-Rh(1)-N(3)	174.1 (3)	C(4)-Rh(2)-N(4)'	93.2 (3)
C(2)-Rh(1)-N(1)	178.7 (3)	C(3)-Rh(2)-N(4)'	175.5 (3)
Ring 1			
C(6)-N(1)-C(9)	105.8 (5)	Ring 2	
N(1)-C(9)-C(10)	108.0 (6)	C(5)-N(3)-C(8)	104.9 (5)
C(9)-C(10)-N(2)	108.0 (6)	N(3)-C(8)-C(7)	108.8 (6)
C(10)-N(2)-C(6)	106.1 (5)	C(8)-C(7)-N(4)	108.5 (6)
N(2)-C(6)-N(1)	112.0 (5)	C(7)-N(4)-C(5)	104.5 (6)
Ring 1-Ring 2			
N(1)-C(6)-C(5)'	131.6 (6)	N(2)-C(6)-C(5)'	116.3 (5)
N(3)'-C(5)'-C(6)	131.4 (5)	N(4)'-C(5)'-C(6)	115.3 (6)
Carbonyls			
Rh(1)-C(1)-O(2)	177.7 (8)	Rh(2)-C(3)-O(3)	178.8 (7)
Rh(1)-C(2)-O(2)	174.7 (7)	Rh(2)-C(4)-O(4)	176.4 (7)

^a Standard deviation for the last significant digit(s) is given in parentheses.

through each imidazole ring to two rhodium atoms. The geometry about each rhodium atom is approximately square planar with the coordination polyhedron defined by two carbon atoms from terminal carbonyl ligands and by two nitrogen atoms from the biimidazole ligands. Intramolecular bond distances and bond angles are presented in Tables V and VI, respectively. Equations of least-squares planes and the dihedral angles between the normals to these planes are listed in Table VII.

The biimidazole dianion consists of two imidazolato rings: ring 1 [N(1), N(2), C(6), C(9), C(10)] and ring 2 [N(3)'

Table VII. Least-Squares Planes^a in Rh₄(CO)₈(BiIm)₂ and Distances of Selected Atoms from the Planes

Plane	Atom	Dist., ^b Å	Plane	Atom	Dist., ^b Å
1	N(1)	0.011	2	N(3)	0.006
	N(2)	-0.007		N(4)	-0.004
	C(6)	-0.003		C(5)	-0.001
	C(9)	-0.015		C(7)	0.008
	C(10)	0.014		C(8)	-0.009
3	Rh(1)	-0.034	4	Rh(2)	0.023
	N(1)	-0.047		N(2)	-0.037
	N(3)	0.061		N(4)'	0.028
	C(1)	0.069		C(3)	0.025
	C(2)	-0.051		C(4)	-0.039

^a Equations defining planes: (1) $-0.311X + 0.645Y - 0.698Z = -2.75$; (2) $-0.302X - 0.696Y - 0.651Z = -4.58$; (3) $-0.993X - 0.017Y - 0.118Z = -2.16$; (4) $-0.319X + 0.731Y - 0.603Z = -1.63$. ^b Perpendicular distance of atom from plane.

N(4)', C(5)', C(7)', C(8)'] bonded through C(5)' and C(6). Each ring is planar with no atom deviating more than 2σ from the best five-atom least-squares plane. The two rings of one BiIm²⁻ ion are nearly coplanar making a dihedral angle of 4.0° with each other. Corresponding dihedral angles of 1.2 and 0° have been observed in [Ni(H₂BiIm)₂(H₂O)₂](NO₃)₂¹¹ and Rh₂(COD)₂(BiIm),¹ respectively.

Each imidazolato ring of the dianion is rotated toward Rh(2) approximately about an axis normal to the plane of the ring and passing through the 2 position of the ring. The N(1)–N(3)' separation, 3.218 (7) Å, and the N(2)–N(4)' separation, 2.625 (7) Å, compared to the inter-ring nitrogen atom separations (2.818 (7) and 2.807 (7) Å) found in the symmetrical dianion geometry of Rh₂(COD)₂(BiIm) reflect this rotation. The "interior" angles about the 2 positions of each ring are N(2)–C(6)–C(5)' = 116.3 (5)^o and N(4)–C(5)'–C(6) = 115.3 (6)^o as compared to the corresponding "exterior" angles, N(1)–C(6)–C(5)' = 131.6 (6)^o and N(3)'–C(5)'–C(6) = 131.4 (5)^o. Similar rotation of imidazole rings in H₂BiIm upon coordination with a metal has been observed in the Ni(II) complex with H₂BiIm.¹¹

The rotation of the imidazole rings toward the coordinating metal reflects the molecular geometry of the biimidazole ligand. The configuration of nitrogen atoms about the C–C bond joining the two imidazole rings is similar to bipyridyl as a bidentate aromatic nitrogen ligand. The pyridine rings of bipyridyl also rotate toward the coordinating metal ion because the N–N "bite" of bipyridyl is too large to allow good overlap of metal and nitrogen orbitals.¹² Similarly, the imidazolato rings of BiIm²⁻ can rotate toward the coordinating metal in order to decrease the inter-ring N–N distance and provide maximum overlap of metal and nitrogen orbitals.

The bond lengths and interior angles for each imidazolato ring of BiIm²⁻ are in the range reported for corresponding values 1.405 – 1.441 Å in other biimidazole structures.^{1,11}

The coordination geometry about Rh(1) is approximately square planar with angles about Rh(1) between the ligands ranging from 89.0 (2) to 92.1 (3)^o with a median of 90.0° . A least-squares plane consisting of Rh(1), C(1), C(2), N(1), and N(3) was calculated and showed deviations of 0.034 – 0.069 Å from that plane. The Rh(1)–N bond lengths of 2.084 (5) and 2.067 (5) Å are shorter than the values 2.120 – 2.141 Å observed in Rh₂(COD)₂(BiIm) and are, in general, somewhat shorter than expected for Rh(I)–N bond lengths. An Rh(I)–N distance of 2.10 Å has been reported for a quinoxalate.¹⁵ However, Rh(III)–N(pyridine) distances range from 2.09 to 2.12 Å.¹⁶ Slightly longer bond lengths might be anticipated for Rh(I)–N due to the larger Rh(I) ionic radius. Rh(1) lies 0.587 Å below the least-squares plane of ring 1 and 0.392 Å below that of ring 2. Similar displacement of the metal from the plane of the imidazolato ring has been reported.^{13,14}

The salient feature of the geometry about Rh(1) is the Rh(1)–Rh(1)' distance of 2.975 (1) Å. This is the shortest Rh(I)–Rh(I) distance known. Rh(I)–Rh(I) distances of 3.02 – 3.18 Å^{17–21} in bridged binuclear structures and 3.14 – 3.31 Å for square planes stacked in a columnar manner^{15,17,22} have been reported and have been described as metal–metal bonds. A metal–metal separation of 2.936 Å in Rh₂(HDMG)₄(PPh₃)₂ has been assigned to a single Rh(II)–Rh(II) bond.²³ The geometry of the BiIm²⁻ ring constrains the Rh(1) atoms to a small range of position in order to maintain maximum overlap of the ligand nitrogen orbitals with the metal orbitals. The relative effects of metal–metal interaction, or bonding, and the constraints imposed by the geometry of the biimidazole ring in determining the Rh–Rh separation cannot be assessed. Nonetheless, the two rhodium atoms do interact strongly and the coordination about each Rh(1) should be described more precisely as five-coordinate with the orbitals of the neighboring rhodium atom occupying the fifth coordination site of each square plane.

The coordination geometry about Rh(2) is a distorted square plane. A least-squares plane consisting of Rh(2), C(3), C(4), N(2), and N(4)' was calculated and revealed deviations of 0.023 – 0.039 Å from that plane. The C(3)–Rh(2)–C(4) angle of 91.3 (3)^o is consistent with square-planar coordination. The N(2)–Rh(2)–N(4)' angle of 78.7 (2)^o, however, departs markedly from square-planar geometry. A similar N–Ni–N angle of 80.7° has been reported in the Ni complex with H₂BiIm.¹¹ As described previously this geometry is presumably required for proper overlap of the nitrogen orbitals with the metal orbitals. The remaining angles of the square plane, N(2)–Rh(2)–C(3) = 96.9 (3)^o and N(4)'–Rh(2)–C(4) = 93.2 (3)^o, merely reflect the N(2)–Rh(2)–N(4)' angle. Rh(2)–N bonds of 2.087 (5) and 2.055 (5) Å are consistent with those about Rh(1). Inequivalent M–N bond lengths to the biimidazole ring have been reported also in [Ni(H₂BiIm)₂]²⁺.¹¹ Bond lengths and angles associated with the carbonyl ligands about Rh(2) are consistent with those for Rh(1) and related carbonyl structures.

The square planes about each Rh(1) atom are twisted 40° away from an eclipsed conformation about an axis joining Rh(1)–Rh(1)'. This is reflected in the staggered carbonyl ligands when viewed along the Rh(1)–Rh(1)' axis and the relative spatial orientation of the BiIm ligands. The rotation of the carbonyl ligands results in the relief of oxygen–oxygen repulsions. If the Rh(1)–Rh(1)' coordination planes were eclipsed, the oxygen–oxygen contacts would be identical with the Rh(1)–Rh(1)' separation, 2.98 Å, which is nearly equal to the sum of the van der Waals radii for oxygen, 3.1 Å.²⁴ As it is, the oxygen–oxygen contact distances are increased to 3.2 Å. This staggering of carbonyl ligands to relieve oxygen–oxygen repulsions has been observed in many polynuclear metal carbonyls.²⁵

The molecular complexes, Rh₄(CO)₈(BiIm)₂, form chains arranged in a "saw-tooth" pattern along the *c* axis, as seen in Figures 3 and 4. The most prominent feature of this packing scheme is the intermolecular interaction of the terminal Rh(2) square planes. An intermolecular Rh(2)–Rh(2) separation of 3.259 (2) Å is identical with that observed in Rh(CO)₂(acac), 3.26 Å,²² suggesting relatively strong metal–metal interaction. The "sawtooth" pattern of the chains resembles the structure of [Rh(CO)₂Cl]₂ in which the intermolecular rhodium separation is 3.31 Å.¹⁷

Discussion

In the light of the crystal structure, the other experimental data can be readily interpreted. The likelihood is high that the tetranuclear structure persists in solution. The solution molecular weight (observed 875 ± 50 ; calculated 900) is consistent with that assignment. The five carbonyl bands in

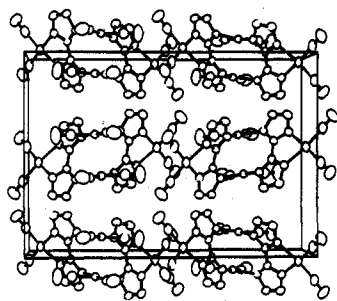


Figure 3. The unit cell of $\text{Rh}_4(\text{CO})_8(\text{BiIm})_2$ viewed along the b axis.

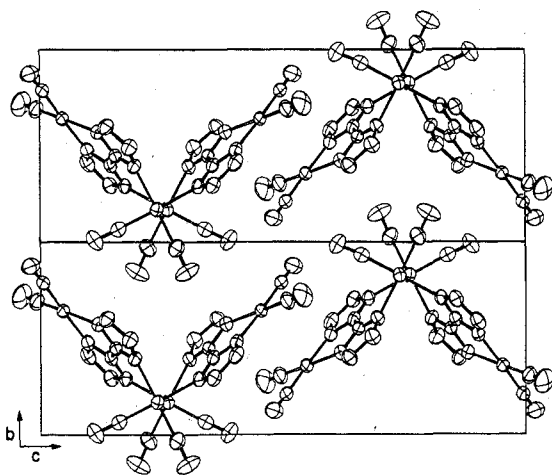
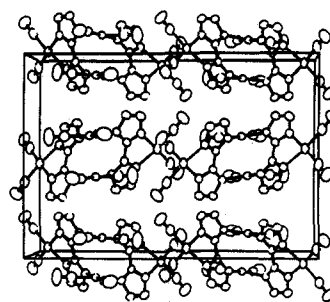


Figure 4. Side view of two chains of $\text{Rh}_4(\text{CO})_8(\text{BiIm})_2$.

the solution ir spectrum may be interpreted with respect to this structure as the summation of a two-band spectrum from the terminal *cis*-dicarbonyl units and a three-band spectrum from the pair of bridging rhodium dicarbonyl units. The three-band portion of the spectrum is typical for complexes containing this "sawhorse" arrangement of four carbonyl ligands, e.g., $\text{Ru}_2(\text{ROO})_2(\text{CO})_4\text{L}_2$.²⁶ In chloroform and other solvents¹ two chemically inequivalent proton resonances are observed, consistent with the tetranuclear configuration. In benzene and toluene, however, an unexplained single resonance was found. The ¹³C NMR spectrum of the enriched carbonyl complex contains two overlapping doublets in the carbonyl region in both toluene and chloroform, again consistent with the tetranuclear configuration. The solution carbonyl stretching bands of the infrared spectrum and the electronic spectrum of the carbonyl complex are independent of solvent.

The corresponding iridium carbonyl complex is assigned the same tetranuclear structure, $\text{Ir}_4(\text{CO})_8(\text{BiIm})_2$, by comparison of the solid-state and solution infrared spectra, the ¹H NMR spectrum, and the electronic absorption spectrum with those of $\text{Rh}_4(\text{CO})_8(\text{BiIm})_2$. The iridium complex exhibits no solvent-dependent behavior.

A structure based upon the tetranuclear configuration of $\text{Rh}_4(\text{CO})_8(\text{BiIm})_2$ is proposed for the mixed-ligand complex $\text{Rh}_4(\text{COD})_2(\text{CO})_4(\text{BiIm})_2$. The two COD ligands would occupy coordination sites about the terminal Rh(2) atoms, Figure 1, and the four CO ligands would coordinate in the same manner as the carbonyl complex about the Rh(1) atoms. Bands associated with BiIm in the solid-state infrared spectrum are nearly identical in position with those of $\text{Rh}_4(\text{CO})_8(\text{BiIm})_2$ and do not indicate formation of the symmetrical BiIm ligand. Bands associated with the coordinated diolefin COD are observed. The solution ir spectrum contains three CO stretching bands at 2090 (s), 2066 (m), and 2022 (s) cm^{-1} , consistent with the arrangement of four CO ligands about the two bridging Rh(1) atoms.²⁶



In the solid state, the molecular complexes $\text{Rh}_4(\text{CO})_8(\text{BiIm})_2$ are arranged in chains (Figures 3 and 4) with an intermolecular Rh–Rh separation of 3.256 Å between the terminal Rh(2) positions. This separation is nearly identical with the Rh–Rh distance observed in $\text{Rh}(\text{CO})_2(\text{acac})$ ²² and suggests that semiconductor behavior might be observed. The electrical resistivity was measured by the two-probe technique on compressed pellets or single crystals using Auquadag contacts to the sample. The conductivity was $<10^{-8} \Omega^{-1} \text{cm}^{-1}$, the lower limit of the equipment, indicating insulating behavior. The value measured for single crystals of $\text{Rh}(\text{CO})_2(\text{acac})$ is $10^{-11} \Omega^{-1} \text{cm}^{-1}$.²⁷

The most prominent feature observed in a comparison of the molecular structures of $\text{Rh}_2(\text{COD})_2(\text{BiIm})$ and $\text{Rh}_4(\text{CO})_8(\text{BiIm})_2$ is the bonding configurations of the BiIm ligand. The reasons for this difference are difficult to ascertain but some comparison can be made with known systems.

$[\text{Rh}(\text{CO})_2\text{Cl}]_2$ exhibits a bent bridged structure reflecting inter- and intramolecular metal–metal bonding.¹⁷ $[\text{Rh}(\text{COD})\text{Cl}]_2$, however, has a strictly planar RhCl_2Rh bridging structure.²⁸ There would be no significant steric repulsion between the terminal COD ligands in a bent structure. In fact, a bent bridged structure has been observed in the mixed-ligand complex $(\text{COD})\text{RhCl}_2\text{Rh}[\text{P}(\text{OPh}_3)]_2$ upon substitution of one COD ligand with triphenyl phosphite.¹⁹

It is also reasonable to assume that the biimidazole dianion adopts the bidentate–monodentate configuration in $\text{Rh}_4(\text{CO})_8(\text{BiIm})_2$ because its "bite", intramolecular N–N distance, is too large for optimum bonding with the rhodium. The rotation of each imidazole ring toward the metal in $\text{Rh}_4(\text{CO})_8(\text{BiIm})_2$ and $[\text{Ni}(\text{H}_2\text{BiIm})_2(\text{H}_2\text{O})_2](\text{NO}_3)_2$ ¹¹ supports this. Metal–metal interaction of the bridging rhodium atoms in $\text{Rh}_4(\text{CO})_8(\text{BiIm})_2$ may be a driving force toward the tetranuclear structure.

It is also possible that changing the terminal ligand from 1,5-cyclooctadiene to carbonyl has so modified the electron density on the rhodium atom that significant changes in molecular geometry are required to stabilize the system. Thus, the bonding configuration of the BiIm ligand and the overall molecular structure of the complex may depend upon a sensitive balance of ligand properties. We are currently exploring these possibilities via syntheses of related derivatives.

Registry No. $\text{Rh}_4(\text{COD})_2(\text{CO})_4(\text{BiIm})_2$, 60195-79-1; $\text{Rh}_4(\text{CO})_8(\text{BiIm})_2$, 60184-36-3; $\text{Ir}_4(\text{CO})_8(\text{BiIm})_2$, 60184-35-2; $\text{Rh}_4(\text{CO})_8(\text{BiIm})_2$, 60184-34-1; $\text{Rh}(\text{COD})(\text{HBiIm})$, 54937-01-8; $\text{Rh}(\text{COD})(\text{acac})$, 12245-39-5; $\text{Rh}(\text{CO})_2(\text{acac})$, 14874-82-9; $\text{Rh}(\text{CO})_2(\text{HBiIm})$, 54936-01-5; $\text{Ir}(\text{CO})_2(\text{acac})$, 14023-80-4; $\text{Rh}_2(\text{COD})_2(\text{BiIm})$, 54937-05-2.

Supplementary Material Available: Listing of structure factor amplitudes (8 pages). Ordering information is given on any current masthead page.

References and Notes

- (1) S. W. Kaiser, R. B. Saillant, W. M. Butler, and P. G. Rasmussen, *Inorg. Chem.*, preceding paper in this issue.
- (2) (a) K. Krogmann, *Angew. Chem., Int. Ed. Engl.*, **8**, 35, (1969); (b) T. W. Thomas and A. E. Underhill, *Chem. Soc. Rev.*, **1**, 99 (1972); (c)

- J. S. Miller and A. J. Epstein, *Prog. Inorg. Chem.*, **20**, 1 (1976); (d) H. R. Zeller, *Festkoerperprobleme*, **13**, 31 (1973).
- (3) S. W. Kaiser, R. B. Saillant, and P. G. Rasmussen, *J. Am. Chem. Soc.*, **97**, 425 (1975).
- (4) S. D. Robinson and B. L. Shaw, *J. Chem. Soc.*, 4997 (1965).
- (5) O. A. Gansow, A. R. Burke, and G. N. La Mar, *J. Chem. Soc., Chem. Commun.*, 456 (1972).
- (6) A. Steyermark, "Quantitative Organic Analysis", The Blackstone Co., New York, N.Y., 1951, p 292.
- (7) J. Chatt and L. M. Venanzi, *J. Chem. Soc.*, 4735 (1957).
- (8) Computations were carried out on an IBM 360/65 computer. Computer programs used during the structural analysis were SYNCOR (data reduction by W. Shmonsees), N. W. Alcock's absorption program, FORDAP (Fourier synthesis by A. Zalkin), ORFLS (full-matrix least-squares refinement by Busing, Martin, and Levy), ORFFE (distances, angles, and their esds by Busing, Martin, and Levy), ORTEP (thermal ellipsoid drawings by C. K. Johnson), HATOMS (hydrogen atom positions by A. Zalkin), and PLANES (least-squares by D. M. Blow).
- (9) D. T. Cromer and J. T. Weber, *Acta Crystallogr.*, **18**, 104 (1965).
- (10) C. H. MacGillavry, G. D. Reich, and K. Lonsdale, "International Tables for X-Ray Crystallography", Vol. III, Kynoch Press, Birmingham, England, 1962, p 201.
- (11) A. D. Mitchell, C. W. Reimann, and F. A. Mauer, *Acta Crystallogr., Sect. B*, **25**, 60 (1969).
- (12) F. S. Stephens, *J. Chem. Soc., Dalton Trans.*, 1350 (1972).
- (13) B. K. S. Lundberg, *Acta Chem. Scand.*, **26**, 3900 (1972).
- (14) G. Ivarsson, B. K. S. Lundberg, and N. Ingri, *Acta Chem. Scand.*, **26**, 3005 (1972).
- (15) L. J. Kuzmina, Yu. S. Varshavskii, N. G. Bokii, Yu. T. Struchkov, and T. G. Cherkesova, *Zh. Strukt. Khim.*, **12**, 653 (1971).
- (16) R. J. Hoare and O. S. Mills, *J. Chem. Soc., Chem. Commun.*, 2138 (1972), and references therein.
- (17) L. F. Dahl, C. Martell, and D. L. Wampler, *J. Am. Chem. Soc.*, **83**, 1761 (1961).
- (18) K. Klanderma and L. F. Dahl, quoted by L. R. Bateman, P. M. Maitlis, and L. F. Dahl, *J. Am. Chem. Soc.*, **91**, 7292 (1969).
- (19) J. Coetzer and G. Gafner, *Acta Crystallogr., Sect. B*, **26**, 985 (1970).
- (20) M. G. B. Drew, S. M. Nelson, and M. Sloan, *J. Chem. Soc., Dalton Trans.*, 1484 (1973).
- (21) J. J. Bonnet, Y. Jeannin, P. Kalck, A. Maisonnat, and R. Poilbanc, *Inorg. Chem.*, **14**, 743 (1975).
- (22) N. A. Bailey, E. Coates, G. B. Robertson, F. Bonati, and R. Ugo, *Chem. Commun.*, 1041 (1967).
- (23) K. G. Caulton and F. A. Cotton, *J. Am. Chem. Soc.*, **93**, 1914 (1971).
- (24) A. Bondi, *J. Phys. Chem.*, **68**, 441 (1964).
- (25) E. W. Abel and F. G. A. Stone, *Q. Rev., Chem. Soc.*, **23**, 325 (1969), and references therein.
- (26) G. R. Crooks, B. F. G. Johnson, J. Lewis, I. G. Williams, and G. Gamlin, *J. Chem. Soc. A*, 2761 (1969).
- (27) C. G. Pitt, L. K. Monteith, L. F. Ballard, J. P. Collman, J. C. Morrow, W. R. Roper, and R. Ulkii, *J. Am. Chem. Soc.*, **88**, 4286 (1966).
- (28) J. A. Ibers and R. G. Snyder, *Acta Crystallogr.*, **15**, 923 (1962).

Contribution from the Department of Industrial Chemistry,
University of Tokyo, Hongo, Tokyo, Japan

Preparation and Properties of Dinitrogen-Molybdenum Complexes. 3.¹

Preparation and Molecular Structure of

1-(η -Hydrazido(2-))fluorobis[1,2-bis(diphenylphosphino)ethane]molybdenum

Tetrafluoroborate-Dichloromethane Solvate,

[Mo(N₂H₂)F(Ph₂PCH₂CH₂PPh₂)₂][BF₄·CH₂Cl₂]

MASANOBU HIDAI,* TERUYUKI KODAMA, MAKI SATO, MICHIHARU HARAKAWA,
and YASUZO UCHIDA

Received March 22, 1976

AC160197D

The compound [Mo(N₂H₂)F(Ph₂PCH₂CH₂PPh₂)₂][BF₄·CH₂Cl₂] was prepared by the reaction of [Mo(N₂)₂(Ph₂PCH₂CH₂PPh₂)₂] with excess aqueous fluoboric acid. The structure of the complex has been determined from three-dimensional x-ray counter data collected on a single crystal. The material crystallizes in space group *D*₂⁴-*P*₂₁₂₁ of the orthorhombic system with four formula units of the complex in a cell of dimensions *a* = 18.966 (7) Å, *b* = 20.740 (7) Å, *c* = 13.362 (5) Å, and *V* = 5256.1 Å³. The structure has been refined by block-diagonal least-squares techniques to a final *R* index of 0.0841 based on 4992 reflections above background. The molybdenum atom has octahedral coordination with Mo-P = 2.541 (3) Å (average), Mo-F = 1.992 (8) Å, and Mo-N(1) = 1.762 (12) Å. The hydrazido(2-) ligand lies in a plane approximately perpendicular to the least-squares plane through the four phosphorus atoms. The N(1)-N(2) bond length is 1.333 (24) Å and the Mo-N(1)-N(2) angle is 176.4 (13)°. A hydrogen bond is observed between the hydrazido(2-) ligand and tetrafluoroborate anion.

Introduction

Recent extensive studies of the reactivity of molybdenum- and tungsten-dinitrogen complexes have disclosed that the end-on coordinated dinitrogen of these complexes reacts with mineral acids, acyl halides, and alkyl halides to give ammonia and several complexes containing a ligand derived from the dinitrogen ligand.² In a previous paper,¹ we reported the preparation of a new series of molybdenum-dinitrogen complexes of the type [Mo(N₂)(RCN)(dpe)₂] (dpe = Ph₂PCH₂CH₂PPh₂), and formation of the benzoylazo complex [MoCl(N₂COPh)(dpe)₂] from their reaction with benzoyl chloride. During the course of our studies on the reactions of these molybdenum-dinitrogen complexes with carbonium salts, we have found that the complex [Mo(N₂H₂)F(dpe)₂][BF₄·CH₂Cl₂] is prepared by the reaction of [Mo(N₂)₂(dpe)₂] with excess aqueous fluoboric acid. Chatt and his co-workers have recently prepared a similar complex [M(N₂H₂)F(dpe)₂][BF₄] (M = Mo or W) from [M(N₂)₂(dpe)₂] (M = Mo or W) and anhydrous fluoboric acid in tetrahydrofuran.³ In this paper we wish to describe the

preparation and the molecular structure of [Mo(N₂H₂)F(dpe)₂][BF₄·CH₂Cl₂].⁴

Experimental Section

All reactions were carried out under an atmosphere of pure nitrogen. Solvents were dried and distilled under nitrogen. [Mo(N₂)₂(dpe)₂] was prepared by the method described in a previous paper.⁵ ³¹P (40.5 MHz), ¹H (100 MHz), and ¹⁹F (94 MHz) spectra were recorded on a computer-assisted JEOL PS-100 spectrometer.

Preparation of [Mo(N₂H₂)F(dpe)₂][BF₄·CH₂Cl₂]. To a solution of [Mo(N₂)₂(dpe)₂] (0.200 g, 0.211 mmol) in tetrahydrofuran (10 ml) was added 48% aqueous HBF₄ (116 μl, 0.850 mmol) at -40 °C. After the mixture was stirred at ambient temperature for about 20 h, addition of *n*-hexane yielded yellowish brown crystals. Recrystallization of these crystals from dichloromethane/*n*-hexane gave orange crystals, which were washed with *n*-hexane and dried in vacuo (0.159 g, 67.8% yield). Anal. Calcd for C₃₃H₅₂N₂BF₅Cl₂P₄Mo: C, 57.2; H, 4.7; N, 2.5; F, 8.5; Cl, 6.4. Found: C, 57.0; H, 4.8; N, 2.2; F, 7.7; Cl, 6.4.

Reaction of [Mo(N₂)₂(dpe)₂] with Et₃O⁺BF₄⁻. To a solution of [Mo(N₂)₂(dpe)₂] (0.480 g, 0.50 mmol) in dichloromethane (17 ml) was added Et₃O⁺BF₄⁻ (0.383 g, 2.0 mmol) at -40 °C. The solution